Integrated Experimental and Computational Methods for Structure Determination and Characterization of a New, Highly Stable Cesium Silicotitanate Phase, $Cs_2TiSi_6O_{15}$ (SNL-A)

M. Nyman,[†] F. Bonhomme,[†] D. M. Teter,[‡] R. S. Maxwell,[§] B. X. Gu,[||] L. M. Wang,[||] R. C. Ewing,[||] and T. M. Nenoff*,[†]

Catalysis and Chemical Technologies Department, MS 0710, and Geochemistry Department, MS 0750, Sandia National Laboratories, P.O. Box 5800, Albuquerque, New Mexico 87185, Analytical and Nuclear Sciences Division, Lawrence Livermore National Laboratory, P.O. Box 808/L-091, Livermore, California 94551, and Department of Nuclear Engineering and Radiological Sciences, University of Michigan, Ann Arbor, Michigan 48109-2104

Received March 27, 2000. Revised Manuscript Received August 11, 2000

Exploratory hydrothermal synthesis in the system $Cs_2O-SiO_2-TiO_2$ has produced a new polymorph of $Cs_2TiSi_6O_{15}$ (SNL-A), whose structure was determined using a combination of experimental and theoretical techniques (^{29}Si and ^{133}Cs NMR, X-ray powder diffraction, and density functional theory). SNL-A crystallizes in the monoclinic space group *Cc* with unit cell parameters $a = 12.998(2)$ Å, $b = 7.5014(3)$ Å, $c = 15.156(3)$ Å, and $\beta = 105.80(3)°$. The SNL-A framework is an unbranched drier single-layer silicate with silicon tetrahedra and titanium octahedra that are linked in 3-, 5-, 6-, 7-, and 8-membered rings in three dimensions. SNL-A is distinctive from a previously reported *C*2/*c* polymorph of $Cs_2TiSi_6O_{15}$ by orientation of the $Si_2O_5^{2-}$ layers and by different ring geometries. Similarities and differences between the two structures are discussed. Other characterizations of SNL-A include TGA-DTA, Cs/Si/Ti elemental analyses, and SEM/EDS. Furthermore, the chemical and radiation durability of SNL-A was studied in interest of ceramic waste form applications. These studies show that SNL-A is durable in both radioactive and rigorous chemical environments. Finally, calculated cohesive energies of the two $Cs_2TiSi_6O_{15}$ polymorphs suggest that the *Cc* SNL-A phase (synthesized at 200 °C) is energetically more favorable than the *C*2/*c* polymorph (synthesized at 1050 °C).

Introduction

We are currently studying the viability of silicotitanate phases for cleanup of radionuclides such as ^{90}Sr and ^{137}Cs. Silicotitanate materials of interest include the following: (1) microporous phases for radionuclide sorption; (2) condensed, leach resistant phases for radionuclide storage. The ^{137}Cs and ^{90}Sr together compose greater than 99% of the radioactive inventory of the Hanford wastes, and removal and immobilization of these radionuclides is a primary goal for remediation of this DOE defense waste site.[1,2] A proprietary ion exchanger material jointly developed by Sandia National Laboratories and Texas A & M University, designated crystalline silicotitanate (CST), is currently the best candidate for ^{137}Cs removal.[3−6] Furthermore, its oxide components are suitable for the matrix of a ceramic waste form. Heat treating Cs-loaded CST up to 1000 °C results in dehydration and subsequent formation of a mixture of crystalline phases which are very resistant to Cs leaching.[7,8] With the interest of studying the unique durability and stability of silicotitanate phases, a collaborative effort between Sandia National Laboratories (SNL) (hydrothermal synthesis and characterization), Pacific Northwest National Laboratory (PNNL) (solid-state synthesis and characterization), and UC Davis (calorimetry studies)[9] is ongoing to carry out phase searches using component oxides of the Cs-loaded CST material. Current investigations include hydrothermal and solid-state synthesis of $Cs_2O-SiO_2-TiO_2$ phases.

* To whom correspondence should be addressed.
[†] Catalysis and Chemical Technologies Department, Sandia National Laboratories.
[‡] Geochemistry Department, Sandia National Laboratories.
[§] Lawrence Livermore National Laboratory.
[||] University of Michigan.

(1) Wilson, E. K. *Chem. Eng. News* **1997**, 300.
(2) Illman, D. L. *Chem. Eng. News* **1993**, 9.
(3) Nenoff, T. M.; Thoma, S. G.; Krumhansl, J. L. *SAND96-2580: The Stability and Selectivity of TAM5: A Silicotitanate Molecular Sieve for Radwaste Clean-up*; Sandia National Laboratories: Albuquerque, NM, 1996.
(4) Poojary, D. M.; Cahill, R. A.; Clearfield, A. *Chem. Mater.* **1994**, *6*, 2364.
(5) Anthony, R. G.; Phillip, C. V.; Dosch, R. G. *Waste Manage.* **1993**, *13*, 503.
(6) Anthony, R. G.; Dosch, R. G.; Gu, D.; Philip, C. V. *Ind. Eng. Chem. Res.* **1994**, *33*, 2702.
(7) Su, Y.; Balmer, M. L.; Wang, L.; Bunker, B. C.; Nenoff, T. M.; Nyman, M.; Navrotsky, A. *Evaluation of Thermally Converted Silicotitanate Waste Forms*; Boston, MA, 1998; p 77.
(8) Su, Y.; Balmer, M. L.; Bunker, B. C. *Evaluation of Cesium Silicotitanates as an Alternative Waste Form*; Boston, MA, 1997; p 457.
(9) Xu, H.; Navrotsky, A.; Nyman, M.; Nenoff, T. M. *J. Mater. Res.* **2000**, *15*, 815.

10.1021/cm000259g CCC: $19.00
Published on Web 10/21/2000

Prior to this collaboration, only one $Cs_2O-SiO_2-TiO_2$ phase had been reported. This phase is a Cs/Si/Ti pharmacosiderite analogue, $HCs_3Ti_4Si_3O_{16}\cdot 4H_2O$, which is a hydrothermally synthesized, microporous ion exchanger.[10,11] The efforts of our studies have added four additional $Cs_2O-SiO_2-TiO_2$ phases which include the following: (a) phases synthesized by solid-state/flux routes at PNNL, $CsTiSi_2O_{6.5}$ (pollucite analogue) and the *C*2/*c* polymorph of $Cs_2TiSi_6O_{15}$;[12−15](b) phases synthesized by hydrothermal routes at SNL, microporous $Cs_3TiSi_3O_{9.5}\cdot 3H_2O$ (SNL-B) [16,17] and the currently reported *Cc* polymorph of $Cs_2TiSi_6O_{15}$ (SNL-A).

The synthesis, structure determination, and characterization of the *Cc* polymorph of $Cs_2TiSi_6O_{15}$ are presented in this report. The focus of this body of work is 4-fold: (1) hydrothermal synthesis of a new $Cs_2O-SiO_2-TiO_2$ phase; (2) the integrated use of three techniques (X-ray Rietveld refinement, density functional theory (DFT), and ^{29}Si and ^{133}Cs solid-state NMR) to determine the correct structure of a complex microcrystalline powder phase with 24 independent atoms in the unit cell; (3) comparison of the structure, stability, physical properties, and synthesis conditions of *Cc* SNL-A to that of the *C*2/*c* polymorph; (4) examination of the theoretical, chemical, and radiation stability of SNL-A, to assess its viability as a waste form phase.

Experimental Section

General Instrumentation. *The X-ray powder diffraction* pattern of $Cs_2TiSi_6O_{15}$ was measured on a Siemens D500 diffractometer with a Ni-filtered Cu Kα radiation. The data were collected over the angular range 5−100° in 2θ with a step size of 0.025° and a counting time of 20 s per step. The front-loaded sample was rotated at 30 rpm during the measurement.

Magic Angle Spinning Nuclear Magnetic Resonance Spectrometry. The ^{133}Cs MAS NMR was acquired at 65.6 MHz (11.7 T) on a Bruker DRX-500 spectrometer using a Bruker 4 mm CP MAS probe. Sample spinning speed was kept constant at 10 kHz. The ^{133}Cs spectrum was recorded at both fields using a 1-pulse acquire experiment with proton decoupling. Pulse lengths were chosen to be approximately one-fourth of a nonselective $\pi/2$ (~8 ms) pulse, though experiments with variable pulse lengths indicated that all peaks could be characterized by the same nutation behavior. Solid cesium chloride (223 ppm) and 0.1 M CsCl (0 ppm) were used for external standardization. A 300 s recycle delay was used, and 192 scans were collected. The ^{29}Si MAS NMR was performed at 99.4 MHz on the same Bruker DRX-500 spectrometer and 4 mm probe. The ^{29}Si MAS NMR spectrum was also acquired with 1 pulse acquire experiments though full nonselective $\pi/2$ pulses of 8.5 ms were used. Neat tetramethylsilane (TMS) was used as an external standard (0 ppm) for the ^{29}Si NMR. A recycle delay of 600 s was used, and 400 scans were collected.

Inductively coupled plasma atomic emission spectroscopy (ICP-AES) for Si and Ti was carried out using an AtomScan-25 ICP-AES instrument, with an argon plasma flame. Samples were dissolved in HF and diluted with water. Reference samples were 10 ppm Si and Ti.

Elemental analysis for Cs by a*tomic adsorption spectroscopy (AAS)* was performed on a Perkin-Elmer 5100 PC AAS instrument. Solutions and standards were prepared with 1000 ppm KCl ionization suppressant. An acetylene/air flame was used for Cs analysis.

The differential thermal analysis−thermogravimetric analysis (DTA−TGA) experiments were performed on a STD 2960 TA DTA−TGA instrument with alumina as a standard for DTA. Samples of SNL-A (10−15 mg) were heated at 5 °C/min to 1400 °C with an argon flow of 20 cm^3/min.

Scanning electron microscopy (SEM) data are collected on a JEOL JSM-T300 SEM with energy dispersive capabilities.

BET surface area measurements were performed on a Quantachrome Autosorb 6B automated gas sorption system, with adsorbed and desorbed volumes of nitrogen at relative pressures in the range 0.05−1.0.

Synthesis of SNL-A. Titanium isopropoxide (TIPT, 0.64 mmol) and tetraethyl orthosilicate (TEOS, 5.1 mmol) were combined by stirring and added dropwise to 50% CsOH solution (5.1 mmol) in a 23 mL Teflon liner for a Parr pressure reactor. After stirring for approximately 30 min, 7.3 mL of H_2O was added and the mixture was stirred for 30 min more. The final pH of the mixture was approximately 12.7 with a final stoichiometry of $Cs:Ti:Si:H_2O = 8:1:8:695$. The Parr pressure reactor was placed in a 200 °C oven and heated for 4 weeks. The product was collected by filtration and washed with hot (80 °C) deionized water.

Cesium Leach Tests. The standard PCT (product consistency test) leach test, a common technique developed to evaluate chemical durability of nuclear waste forms in aqueous environments,[18,19] was performed on SNL-A. A sample of the material (0.2 g) was placed in a hydrothermal bomb with 10 g of water at 90 °C for 1, 2, 3, 7, and 10 days. After the designated time of heating, each sample was filtered and the leachate solution was analyzed for Cs concentration by AAS. The solid product was analyzed by XRD to determine if any phase changes had occurred. Surface area of samples for leach rate calculations was determined by BET measurements (29 m^2/g).

Electron Irradiation Studies. Electron irradiation studies of SNL-A were conducted with a JEOL 2000FX transmission electron microscope (TEM) at the University of Michigan. The electron energy used was 200 keV, and the sample was irradiated at a dose rate of 5×10^{23} electrons/(s·cm^2).

Results and Discussion

Synthesis of SNL-A. Approximately 0.3 g (0.42 mmol) of SNL-A was collected from the synthesis reaction described above. This corresponds with a 66% yield based on TIPT, the limiting reagent in the synthesis reaction. The reaction is also directly scaleable to obtain more product by utilizing a larger Parr pressure reactor (125 mL Teflon liner). Wet chemical analysis for Ti (ICP-AES), Si (ICP-AES), and Cs (AA) gave 24.5 wt % Si (calcd 23.3 wt %), 6.77 wt % Ti (calcd 7.25 wt %), and 38.3 wt % Cs (calcd 36.8 wt %). Within experimental error of the analysis techniques (approximately ±5%), the product is pure with the stoichiometry $Cs_2TiSi_6O_{15}$. SEM images of SNL-A are shown in Figure 1a,b. Figure 1a (1000× magnification) shows the uniformity of the crystallite size and the purity of the sample. Figure 1b (3500× magnification) shows the irregular shape of the crystallites, which are approxi-

(10) Behrens, E. A.; Poojary, D. M.; Clearfield, A. *Chem. Mater.* **1996**, *8*, 1236.
(11) Behrens, E. A.; Clearfield, A. *Microporous Mater.* **1997**, *11*, 65.
(12) Balmer, M. L.; Su, Y.; Grey, I. E.; Santoro, A.; Roth, R. S.; Huang, Q.; Hess, N.; Bunker, B. C. *The Structure and Properties of Two New Silicotitanate Zeolites*; Boston, MA, 1997; p 449.
(13) Balmer, M. L.; Huang, Q.; Wong-Ng, W.; Roth, R. S.; Santoro, A. *J. Solid State Chem.* **1997**, *130*, 97.
(14) Grey, I. E.; Roth, R. S.; Balmer, M. L. *J. Solid State Chem.* **1997**, *131*, 38.
(15) McCready, D. E.; Balmer, M. L.; Keefer, K. D. *Powder Diffract.* **1997**, *12*, 40.
(16) Nyman, M.; Gu, B.; Wang, L.; Ewing, R. C.; Nenoff, T. M. *J. Microporous Mesoporous Mater.* **2000**, in press.
(17) Nyman, M.; Nenoff, T. M.; Su, Y.; Balmer, M. L.; Navrotsky, A.; Xu, H. *New Crystalline Silicotitanate (CST) Waste Forms: Hydrothermal Synthesis and Characterization of Cs-Si-Ti-O Phases*; Boston, MA, 1998; p 71.
(18) Li, H.; Tomozawa, M. *J. Non-Cryst. Solids* **1996**, *195*, 188.
(19) Mesko, M. G.; Day, D. E. *J. Nucl. Mater.* **1999**, *273*, 27.

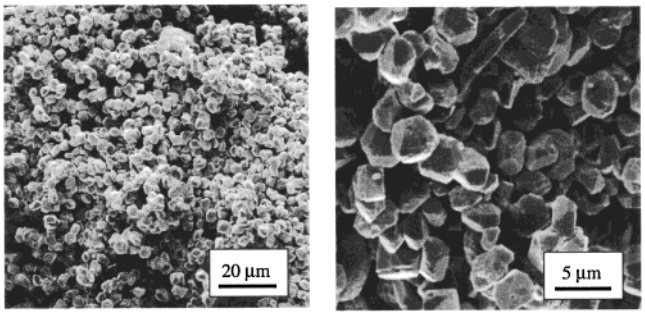

Figure 1. Scanning electron micrographs of SNL-A at 1000× magnification (left), showing the uniformity and purity of the sample; and 3500× magnification (right), illustrating the irregular crystallite shape.

mately 2−5 μm in diameter. No other phases were observed by SEM, which lends further evidence to the formation of a pure material.

Analysis by DTA−TGA revealed a weight loss of less than 1% upon heating to 1400 °C, which indicates SNL-A contains no volatile components such as water molecules or hydroxyl ions. No phase changes were observed by DTA, except an endothermic melting at 1150 °C, which is a similar melting temperature observed for the PNNL *C*2/*c* polymorph of $Cs_2TiSi_6O_{15}$.[20] Upon cooling, SNL-A does not recrystallize; rather, it solidifies as a glassy material. Furthermore, SNL-A does not undergo any solid-state phase transformations up to its melting point, which suggests it is an extremely stable framework. Additionally, SNL-A heated at 1000 °C for 8 h did not show any change in its X-ray diffraction pattern, which is indicative of stability over time at elevated temperatures.

In contrast to the low-temperature hydrothermal conditions under which SNL-A was obtained, the PNNL *C*2/*c* polymorph was synthesized at extremely high temperatures (1000−1100 °C).[14,20] However, since SNL-A does not convert to the PNNL phase by heating, the two polymorphs are not considered low- and high-temperature forms. In this study, the energetics of the two phases are compared by DFT total energy calculations (discussed below). Furthermore, calorimetry studies on the two $Cs_2TiSi_6O_{15}$ polymorphs are currently being carried out with Navrotsky et al. and will give more insight into the relative stability of these phases.

Structure Determination and Refinement. Since no single crystal of sufficient size could be grown, the structure of SNL-A was solved ab initio from X-ray powder diffraction data. From these data, the positions of the first 20 Bragg peaks (corrected with Si as external standard) were used for the indexation with the programs TREOR90[21] and DICVOL91.[22] A satisfactory solution was found in the monoclinic system with cell parameters $a = 12.97(2)$ Å, $b = 7.500(4)$ Å, $c = 15.153(5)$ Å, and $\beta = 105.73(6)$ °, which are similar to those reported for the PNNL phase ($a = 13.386(5)$ Å, $b = 7.423(3)$ Å, $c = 15.134(5)$ Å, $\beta = 107.71(3)$°[14]). The figure of merit[23] obtained from this solution was $F(20) = 15$. The extinction laws were consistent with the space groups *Cc* or *C*2/*c*. The number of independent Cs and Si sites revealed by the NMR data (2 and 6, respectively) was only consistent with a structure described in the noncentrosymmetric space group *Cc*. The correctness of the cell and extinction laws were checked by a full pattern fitting using the Le Bail method,[24] as implemented in the program FULLPROF.[25] No peak was left unaccounted for, thus establishing the validity of the cell and the purity of the sample. The extracted integrated intensities of the peaks below $2\theta = 50°$ were used to solve the structure in the space group *Cc* by direct methods with the program SIR92,[26] incorporated in the Wingx[27] suite.

The positions of the cesium atoms and several of the non-oxygen atoms were directly revealed. The correct assignment of atom types and the completion of the structure were achieved by successive Rietveld refinements using the WinMprof program,[28] difference Fourier analysis and "manual" model-building. Although the framework characteristics and topology of the fully refined structure appeared to be essentially correct, the completely free Rietveld refinement of the 70 free atomic positional parameters led to an unreasonably broad range of Si−O distances, ranging from 1.34 to 1.82 Å with a mean value of 1.59 Å and a standard mean error of 0.13 Å. This imprecision on the oxygen atom positions is partly due to the relative complexity of the structure (24 independent atoms and 70 free positional parameters) and to the strong scattering of the cesium atoms, which tends to dominate the contribution of the Si−Ti−O framework.

To obtain a more reasonable structure in the space group *Cc* than that achieved by the original free Rietveld refinement as described above, two different approaches were used. The first approach was a Rietveld refinement with soft constraints applied on all 24 independent Si−O distances (Si−O = 1.60(2) Å). This constrained refinement of the atomic and profile parameters (91 parameters all together) proceeded smoothly down to very satisfactory agreement indices ($R_{Bragg} = 3.37\%$, $R_p = 11.73\%$, $\chi^2 = 7.62$). No preferred orientation correction was necessary. The atomic displacement parameters were refined isotropically and constrained to be equal for atoms of the same element. The population parameters of the Cs sites were refined in the initial stages of the process and were found to be equal to unity within standard deviations. Therefore, Cs population parameters were hereafter fixed at 100%. Furthermore, no disorder on the Si/Ti sites was evidenced. In comparison with the free refinement, the average shift of the Ti/Si and O atoms from their original positions are 0.05 and 0.12 Å respectively, and the Cs atoms are essentially unshifted.

The second approach used was to optimize the atomic coordinates by minimizing the energy of the structure. This work was carried out by density function theory

(20) Su, Y. Personal communication.
(21) Werner, P. E.; Eriksson, J.; Westdahl, J. *J. Appl. Crystallogr.* **1985**, *18*, 367.
(22) Boultif, A.; Louer, D. *J. Appl. Crystallogr.* **1991**, *24*, 987.
(23) Smith, G. S.; Snyder, R. L. *J. Appl. Crystallogr.* **1979**, *12*, 60.
(24) LeBail, A.; Duroy, H.; Fourquet, J. *Mater. Res. Bull.* **1988**, *23*, 447.
(25) Rodriguez-Carvajal, J. *Collected Abstracts of Powder Diffraction Meeting*; Toulouse, France, 1990; p 127.
(26) Altomare, A.; Cascarano, G.; Giacovazzo, C.; Guagliardi, A.; Burla, M. C.; Polidori, G.; Carnalli, M. *J. Appl. Crystallogr.* **1994**, *27*, 435.
(27) Farrugia, L. J. *J. Appl. Crystallogr.* **1999**, *32*, 837.
(28) Jouanneaux, A. *CPD Newslett.* **1999**, *21*, 13.

(DFT) using the VASP code developed at the Institut fur Theoretische Physik of the Technische Universitat Wien.[29−32] The quantum mechanical modeling of SNL-A is a computationally demanding task. The problems of deep pseudopotentials required to accurately model the oxygen ion, combined with the low symmetry and large unit cell, would have made these calculations intractable until recently.

The electronic degrees of freedom were minimized using a residual minimization method direct inversion in the iterative subspace (RMM-DIIS) algorithm.[33,34] The program solved for the electronic charge density using a density functional framework[35,36] within the local density approximation to electron exchange and correlation. The exchange correlation term of the total energy is the Perdew and Zunger parametrization[37] of the Ceperley and Alder data.[38] The electronic wave functions were expanded in a plane wave basis set with periodic boundary conditions. Vanderbilt ultrasoft pseudopotentials were used for the cesium, titanium, and oxygen ions with the following states being treated as valence electrons: Cs, $5p^6\ 6s^1$; Ti, $3p^6\ 3d^2\ 4s^2$; O, $2s^2\ 2p$.[4] A norm-conserving pseudopotential was used for silicon with the $3s^2\ 3p^2$ states being treated as valence. The internal coordinates of the initial unit cell derived from the free Rietveld refinement were optimized while keeping the unit cell and cesium ions fixed because of the very low experimental uncertainties on these structural constraints ($R_{\mathrm{Bragg}} = 3.20\%$). These calculations resulted in optimization of the framework atoms to obtain the most reasonable Si−O/Ti−O bond distances of the three *Cc* models.

Although the DFT calculations and the constrained Rietveld refinement gave a structurally sensible model, the exact symmetry still required further confirmation. For instance, the positions of the non-oxygen atoms can be approximately described in the centrosymmetric space group *C*2/*c*. Using the positions of the Cs, Ti, and Si atoms from the noncentrosymmetric *Cc* (DFT-optimized) model, we located a pseudo center of symmetry at the position (0.022, 0.001, 0.143) (program MISSYM[39]). The pairs of independent atoms which are approximately related by this pseudo center of symmetry are listed in Table 1. To quantify the overall deviation from centrosymmetry, we calculated for each of these pairs (X1, X2), the distance between X2 and X1′, where X1′ is the inversion of X1 through the pseudo center of symmetry. These distances are also given in Table 1. The O4 is excluded from Table 1 because it is located only 0.47 Å from the pseudo center of symmetry and, therefore, does not have a pseudo-symmetry-related counterpart. Although the arrangement of the Cs atoms is indeed centrosymmetric within experimental errors (deviation of 0.03 Å), the arrangement of the Ti, Si, and especially the O atoms deviates significantly from centrosymmetry. Further confirmation of the *Cc* space group assignment was aided by a Rietveld refinement in the *C*2/*c* supergoup. This refinement yielded acceptable agreement indices but inferior to those of the *Cc* model. Table 2 shows a comparison of those indices for (1) the *C*2/*c* model with Si−O constraints, (2) the unconstrained *Cc* model, (3) the *Cc* model with Si−O constraints, and (4) the DFT-optimized *Cc* model with Cs and unit cell fixed. Figure 2 shows the observed diffraction pattern for SNL-A, along with the difference patterns (with 20× magnification of the vertical scale) for the Si−O distance-constrained *C*2/*c* and *Cc* refine- ments. The *C*2/*c* model gives an unsat-

Table 1. Displacement (Å) of Atoms from Centrosymmetry

atom pair (X1, X2) related by pseudo center of sym	dist between X2 and X1′[a]	atom pair (X1, X2) related by pseudo center of sym	dist between X2 and X1′[a]
Cs1, Cs2	0.028	O1, O13	1.151
Ti1, Ti1	0.409	O3, O3	0.796
Si1, Si2	0.573	O10, O15	0.450
Si4, Si5	0.441	O6, O8	0.696
Si3, Si6	0.341	O7, O7	0.776
O9, O5	0.185	O12, O14	1.074
O2, O11	0.773		

[a] X1′ is defined as the inversion of X1 through the pseudo center of symmetry at (0.022, 0.001, 0.143).

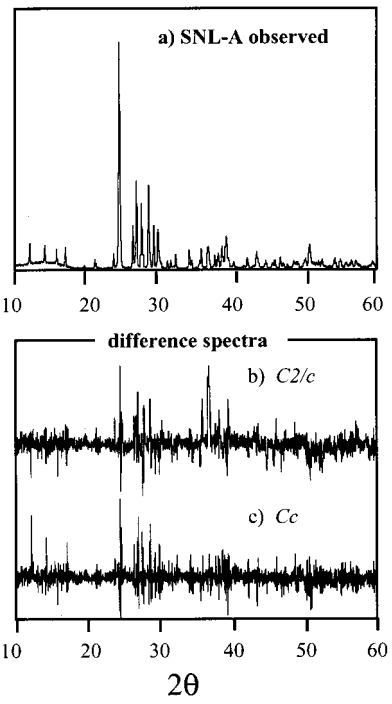

Figure 2. Observed X-ray diffraction pattern for SNL-A (a) and comparison of the difference profiles for the Rietveld refinement of SNL-A in the *C*2/*c* (b) and *Cc* (c) space groups. The difference profiles have a vertical magnification of 20× so distinctions between the *Cc* model and *C*2/*c* models can be observed. A better fit is obtained from the *Cc* model, particularly in the regions $2\theta = 27-30°$ and $35-40°$.

Table 2. Comparison of Agreement Indices

model	R_{bragg}	R_{p}	R_{wp}	χ^2
*C*2/*c* with SiO constraints	6.83	14.36	18.28	10.05
unconstrained *Cc*	3.20	11.63	15.56	7.53
Cc with SiO constraints	3.37	11.73	15.69	7.62
DFT-optimized *Cc* with Cs posns and unit cell fixed	4.53	12.53	16.37	8.05

(29) Kresse, G.; Furthmuller, J. *Comput. Mater. Sci.* **1996**, *6*, 15.
(30) Kresse, G.; Hafner, J. *Phys. Rev. B* **1993**, *47*, 558.
(31) Kresse, G.; Hafner, J. *Phys. Rev. B* **1994**, *49*, 14251.
(32) Kresse, G.; Furthmuller, J. *Phys. Rev. B* **1996**, *54*, 11169.
(33) Pulay, P. *Chem. Phys. Lett.* **1980**, *73*, 393.
(34) Wood, D. M.; Zunger, A. *J. Phys. A* **1985**, *18*, 1343.
(35) Hohenberg, P.; Kohn, W. *Phys. Rev.* **1964**, *136*, 864.
(36) Kohn, W.; Sham, L. J. *Phys. Rev.* **1965**, *140*, 1133.
(37) Perdew, J. P.; Zunger, A. *Phys. Rev. B* **1981**, *23*, 5048.
(38) Ceperley, D. M.; Alder, B. J. *Phys. Rev. Lett.* **1980**, *45*, 566.
(39) LePage, Y. *J. Appl. Crystallogr.* **1987**, *20*, 264.

Table 3. Crystallographic Data for SNL-A

chem formula	$Cs_2TiSi_6O_{15}$
molar mass (g/mol)	722.2
cryst system	monoclinic
space group	*Cc* (No. 9)
a (Å)	12.988(2)
b (Å)	7.5014(3)
c (Å)	15.156(3)
β (deg)	105.80(3)
V (Å^3)	1420.8(7)
Z	4
d_c (g/cm^3)	3.376
λ (or wavelength)	Cu Kα_1, Kα_2
geometry	Bragg−Brentano
range 2θ (deg)	5.00−100.00
Step size (deg)	0.025
Time/ step (s)	20
no. of free params	91[a]
no. of structural params	74[b]
no. of "independent" reflcns	736
no. of soft constraints	24
Min FWHM (deg)	0.11
R_{Bragg} (%)	3.37
R_{wp} (%)	15.69
χ^2	7.62

[a] 74 structural parameters plus 17 profile parameters (cell parameters, pseudo-Voigt mixing parameter, background, asymmetry, etc.). [b] 70 positional parameters (*x*, *y*, *z*) plus 4 isotropic temperature factors.

isfactory fit in the regions $2\theta = 27-30°$ and $2\theta = 35-40°$. Furthermore, the temperature factor for oxygen atoms from the *C*2/*c* model (~8 Å^2) is much greater than that from the *Cc* model (~3 Å^2; see Table 4 footnote). This result lends further evidence that the centrosymmetric model is inadequate in describing SNL-A.

Although the free *Cc* Rietveld refinement gave the best agreement indices due to the greatest degrees of freedom on the model, this data set is disregarded for the remainder of the discussion, due to the unreasonable Si−O distances. The crystallographic data and refinement conditions for the "distance constrained" refinement are presented in Table 3. The structural parameters for two models are given in Table 4: (1) Rietveld refinement with Si−O constraint; (2) DFT structural optimization with Cs position and cell parameters fixed. Although atomic positions are very similar for both models, the DFT model gave a more reasonable range of Ti−O distances (1.917−1.976 Å) than the Rietveld model with Si−O constraint (1.84(3)−2.08(3) Å). Selected interatomic distances and bond angles from the Rietveld model with Si−O constraint are given in Table 5.

Description of Framework and Comparison to the PNNL Polymorph. The calculated powder diffraction patterns of SNL-A and the PNNL $Cs_2TiSi_6O_{15}$ phases are shown in Figure 3 for comparison. Differences between the diffraction patterns are apparent, confirming these are two distinct polymorphs of $Cs_2TiSi_6O_{15}$. SNL-A has six crystallographically unique Si sites, one unique Ti site, and two unique Cs sites. The PNNL phase is of higher symmetry with three unique Si sites, one unique Ti site, and one unique Cs site. For both phases, the TiO_6 octahedron shares six corners with SiO_4 tetrahedra, and each SiO_4 tetrahedron is corner-sharing with one TiO_6 octahedron and three other SiO_4 tetrahedra.

Using Liebau's classification scheme of silicates,[40] SNL-A (and also the PNNL phase) is described as an unbranched dreier single-layer silicate, similar to that observed in synthetic $H_2NaNd[Si_6O_{15}]\cdot nH_2O$.[41] The $Si_2O_5^{2-}$ silicate layers are stacked along the *c*-axis and are corrugated sheets composed of alternating chains of five-membered SiO_4 rings and eight-membered SiO_4 rings (Figures 4 and 5). The edge-on views of the layers (Figure 5) reveal the major architectural difference between the two polymorphs: the layers in the PNNL phase are all oriented in the same direction within the (110) plane, whereas successive layers in SNL-A are related by a 90° rotation within the (110) plane.

The differences and similarities between the ring structures of SNL-A and the PNNL phase are summarized in Table 6. Both phases contain (1) a three-membered ring consisting of one TiO_6 octahedron and two SiO_4 tetrahedra (Figure 6), (2) an eight-membered ring consisting of all SiO_4 tetrahedra (Figures 4 and 6), (3) a five-membered ring composed of four SiO_4 tetrahedra and one TiO_6 octahedron (Figure 7), (4) a five-membered ring composed of five SiO_4 tetrahedra (Figure 4), and (5) a six-membered rings of four SiO_4 tetrahedra and two TiO_6 octahedra (Figure 7). The SNL-A and PNNL polymorphs differ by a seven-membered ring (two TiO_6 octahedra and five SiO_4 tetrahedra) for SNL-A and an eight-membered ring (two TiO_6 octahedra and six SiO_4 tetrahedra) for the PNNL phase (both viewed in Figure 6).

For both phases, the shortest Cs−Cs distances are observed within the channels formed by the eight-member (SNL-A, PNNL) and seven-member (SNL-A) rings. For SNL-A, Cs2 and Cs1 alternate with slightly varying distances of 4.685(2), 5.105(2), and 4.679(2) Å. In comparison, the shortest Cs−Cs distances reported for the PNNL phase are 3.765(2) and 4.904(2) Å.

^{29}Si and ^{133}Cs MAS NMR. Solid-state ^{29}Si and ^{133}Cs MAS NMR analyses of a pure sample of SNL-A gave 6 peaks and 2 peaks, respectively (Figure 8). The 6 Si peaks are all of approximately equal integrated area. The 2 Cs peaks also give a 1:1 peak area ratio. These results played a pivotal role in the final solving and refinement of the structure in the *Cc* space group (6 Si and 2 Cs per asymmetric unit) rather than *C*2/*c* space group (3 Si and 1 Cs per asymmetric unit). The ^{29}Si chemical shifts observed for six unique sites range from −96.8 to −110.0 ppm, which is an unusually large shift range for all Q^3 sites (3 Si, 1 Ti). Furthermore, by conventional Q^x peak assignments, the peak at −110.0 ppm is usually assigned the Q^4 designation[42] and, therefore, might be construed as an impurity peak. Given these unusual features of the NMR data and the important role these data served in the structure determination, further evaluation was necessary. To confirm all six ^{29}Si peaks belong to SNL-A, we calculated ^{29}Si shifts using empirical equations first reported by

(40) Liebau, F. *Structural Chemistry of Silicates*; Springer-Verlag: Berlin, 1985; p 154.
(41) Karpov, O. G.; Pushcharovskii, D. Y.; Pobedimskaya, E. A.; Burshtein, I. F.; Belov, N. V. *Sov. Phys. Dokl.* **1977**, *22*, 464.
(42) Balmer, M. L.; Bunker, B. C.; Wang, L. Q.; Peden, C. H. F.; Su, Y. *J. Phys. Chem. B* **1997**, *101*, 9170.

Table 4. Structural Parameters for Two *Cc* Models

	Rietveld refinement with Si−O constraints (1.60(2) Å) [a]			DFT model using unit cell and Cs coords from the free Rietveld refinement		
atom	*x*(esd)	*y*(esd)	*z*(esd)	x	y	z
Cs1	0.25970 (fixed)	0.3658(8)	0.48146 (fixed)	0.259 70	0.367 10	0.481 46
Cs2	0.2832(3)	0.1337(8)	0.8030(3)	0.284 40	0.134 50	0.804 06
Ti	0.539(1)	0.240(1)	0.400(1)	0.537 40	0.242 15	0.401 10
Si1	0.006(1)	0.068(2)	0.249(1)	0.001 10	0.070 82	0.252 06
Si2	0.057(1)	0.032(2)	0.563(1)	0.051 77	0.027 96	0.565 66
Si3	0.084(1)	0.444(2)	0.242(1)	0.083 08	0.452 08	0.241 43
Si4	0.257(1)	0.113(2)	0.056(1)	0.252 45	0.120 34	0.053 32
Si5	0.322(1)	0.328(2)	0.241(1)	0.317 68	0.342 26	0.240 53
Si6	0.484(1)	0.074(2)	0.039(1)	0.478 98	0.072 57	0.036 24
O1	0.000(2)	0.124(4)	0.002(1)	0.000 00	0.131 27	0.000 00
O2	0.015(2)	0.282(3)	0.261(2)	0.010 25	0.286 33	0.258 21
O3	0.051(2)	0.499(5)	0.136(2)	0.048 66	0.508 03	0.135 32
O4	0.051(2)	0.004(5)	0.166(2)	0.049 79	0.004 08	0.170 55
O5	0.183(2)	0.043(4)	0.576(2)	0.179 49	0.045 11	0.572 25
O6	0.207(2)	0.376(4)	0.262(2)	0.205 23	0.381 97	0.261 71
O7	0.298(2)	0.230(5)	0.146(2)	0.298 46	0.224 00	0.149 11
O8	0.360(2)	0.032(3)	0.027(2)	0.353 42	0.030 45	0.026 47
O9	0.381(2)	0.516(4)	0.236(2)	0.371 90	0.529 47	0.221 41
O10	0.399(2)	0.246(4)	0.332(2)	0.390 77	0.244 24	0.328 00
O11	0.492(2)	0.288(3)	0.030(2)	0.491 62	0.286 87	0.030 43
O12	0.521(2)	0.022(3)	0.461(2)	0.514 37	0.019 81	0.455 38
O13	0.564(2)	0.472(3)	0.341(1)	0.558 30	0.472 40	0.345 01
O14	0.581(2)	0.112(3)	0.304(2)	0.580 85	0.113 15	0.308 08
O15	0.698(2)	0.255(3)	0.478(2)	0.687 31	0.255 73	0.472 77

[a] Isotropic temperature factors: B(Cs) = 3.4 (1) Å^2; B(Ti) = 1.9 (2) Å^2; B(Si) = 1.6 (1) Å^2; B(O) = 3.2 (2) Å^2.

Table 5. Selected Bond Angles and Distances for SNL-A from the Rietveld Refinement with Si−O Constraints (1.60(2) Å)

atom A	O(x)$_1$	A−O(x)$_1$ bond length (Å) (esd)	O(x)$_2$	O(x)$_1$−A−O(x)$_2$ bond angle (deg) (esd)	atom A	O(x)$_1$	A−O(x)$_1$ bond length (Å) (esd)	O(x)$_2$	O(x)$_1$−A−O(x)$_2$ bond angle (deg) (esd)
Ti	O1	1.97(3)	O10	89.6(1.5)	Si3	O2	1.59(2)	O3	111.5(2.1)
	O10	1.84(3)	O12	93.4(1.3)		O3	1.59(2)	O6	104.8(1.8)
	O12	1.92(3)	O14	92.4(1.2)		O6	1.62(2)	O14	109.0(1.8)
	O13	2.02(3)	O14	89.0(1.3)		O14	1.58(2)	O2	113.1(1.8)
	O14	1.95(3)	O15	90.7(1.4)		O2		O6	107.7(1.9)
	O15	2.08(3)	O1	88.3(1.3)		O3		O14	110.4(2.0)
	O1		O12	89.2(1.4)	Si4	O7	1.59(2)	O8	109.3(1.8)
	O1		O13	89.4(1.2)		O8	1.62(2)	O5	111.0(1.8)
	O10		O13	88.8(1.3)		O5	1.60(2)	O15	114.2(1.8)
	O10		O14	91.3(1.4)		O15	1.58(2)	O7	106.3(2.1)
	O12		O15	90.7(1.2)		O7		O5	108.2(2.3)
	O13		O15	87.1(1.2)		O8		O15	107.8(1.9)
Si1	O2	1.61(2)	O4	111.3(2.2)	Si5	O6	1.64(2)	O7	108.3(1.9)
	O4	1.60(2)	O9	113.7(2.0)		O7	1.57(2)	O9	109.7(2.1)
	O9	1.62(2)	O13	102.6(1.7)		O9	1.62(2)	O1	100.5(1.8)
	O13	1.58(2)	O2	110.1(1.8)		O10	1.58(2)	O6	108.4(2.0)
	O2		O9	106.7(1.6)		O6		O9	106.8(1.7)
	O13		O4	111.9(1.8)		O7		O10	122.0(2.1)
Si2	O5	1.60(2)	O11	115.6(1.8)	Si6	O8	1.62(2)	O11	105.3(1.6)
	O11	1.60(2)	O1	108.2(1.8)		O11	1.62(2)	O3	113.8(2.2)
	O1	1.58(2)	O4	110.5(2.2)		O3	1.59(2)	O12	109.7(1.9)
	O4	1.60(2)	O5	102.1(1.8)		O12	1.56(2)	O8	108.8(1.7)
	O5		O1	113.5(1.8)		O8		O3	108.2(1.8)
	O11		O4	106.7(2.2)		O11		O12	110.8(2.0)

CsO Distances (Å)

Cs1	O(x)	dist	O(x)	dist	Cs2	O(x)	dist	O(x)	dist
	O1	3.07(3)	O9	3.85(3)		O2	3.30(3)	O9	3.20(3)
	O2	3.99(3)	O10	3.88(4)		O4	3.33(3)	O10	3.20(3)
	O5	3.11(3)	O11	3.89(3)		O5	3.40(3)	O11	3.93(3)
	O6	3.21(3)	O12	3.26(3)		O6	3.82(3)	O12	3.55(3)
	O7	3.88(4)	O14	3.56(3)		O7	3.66(4)	O13	3.16(3)
	O8	3.25(3)	O15	3.02(2)		O8	3.36(3)	O14	3.24(3)
								O15	3.24(2)

Sherriff [43] and later used specifically for silicotitanates by Laboriau.[44] The ^{29}Si peak shifts were calculated using structural parameters from (a) the Si−O constrained *Cc* model and (b) the DFT-optimized *Cc* model of SNL-A. These results, along with key structural parameters in the equations, namely the Si(x)−O−Si average bond angle and Si(x)−O−Ti bond angle (x = 1−6) are summarized in Table 7. In general, the downfield shift increases with increasing average Si(x)−O−X (X = Si, Ti) angle, especially the average Si(x)−O−Si bond angle. The data from the DFT-optimized *Cc* model gave calculated chemical shifts which agree very well with the observed shifts, and the peaks were assigned to

(43) Sherriff, B. L.; Grundy, H. D. *Nature* **1988**, 819.
(44) Labouriau, A.; Higley, T. J.; Earl, W. L. *J. Phys. Chem.* **1998**, *102*, 2897.

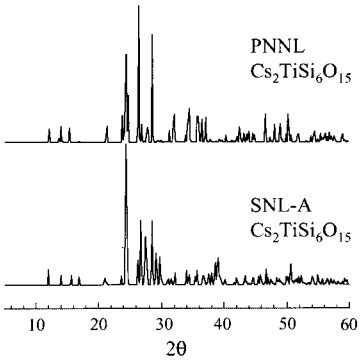

Figure 3. Calculated diffraction patterns for SNL-A (bottom) and the PNNL (top) polymorphs of $Cs_2TiSi_6O_{15}$.

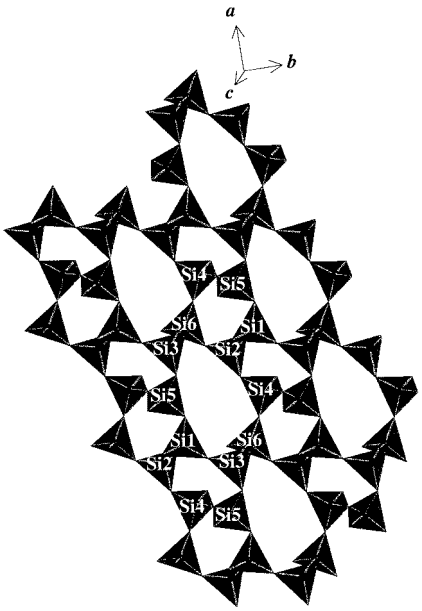

Figure 4. View of SNL-A approximately down the *c*-axis, showing the corrugated $Si_2O_5^{2-}$ layers composed of alternating chains of five-membered SiO_4 rings and eight-membered SiO_4 rings. The Cs atoms are removed for ease of viewing.

crystallographic sites on the basis of these data (see Table 7, column 1). The better agreement between the observed and calculated shifts obtained from the DFT-optimized data confirms that this model provides more optimum atomic positions than the Si−O-constrained Rietveld refinement model. Finally, these results show that the large chemical shift range observed for chemically similar (Q^3, 3 Si, 1 Ti) sites is expected, based on the large range of Si−O−X (X = Si, Ti) bond angles within the framework of SNL-A.

The ^{133}Cs MAS NMR spectrum (Figure 8b) which shows two unique chemical sites in a 1:1 ratio also agrees with the structural solution in the *Cc* space group rather than the *C*2/*c* space group. Cs1 is surrounded by 12 oxygen atoms in the first coordination sphere, and the average Cs−O distance is 3.5 Å. Cs2 is surrounded by 13 oxygen atoms in the first coordination sphere, and the average Cs−O distance is 3.4 Å. The ^{133}Cs NMR chemical shifts are affected by shielding of the Cs by neighboring atoms, where, in general, downfield shifts correlate with decreased shielding.[45−47] This suggests the peak at 69.4 ppm corresponds with the Cs2, which has longer Cs−O distances, and the peak at 91.8 ppm corresponds the Cs1 with shorter Cs−O bond distances.

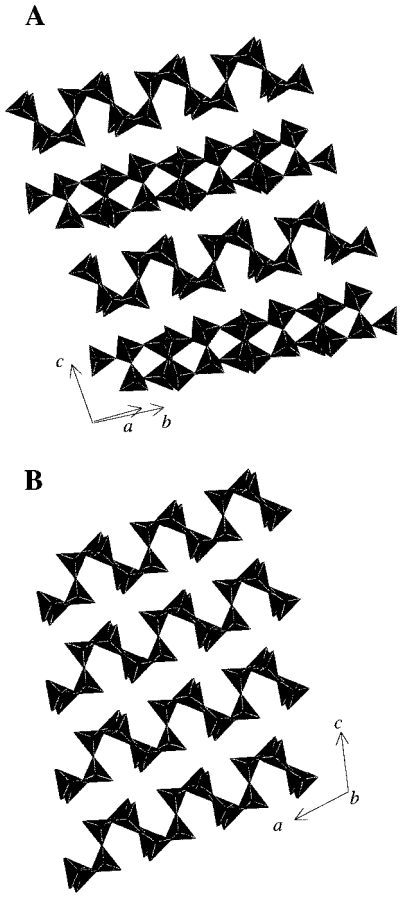

Figure 5. Edge view of the $Si_2O_5^{2-}$ layers in SNL-A (a) and the PNNL phase (b). The Cs and Ti atoms are removed for clarity.

Stability of SNL-A. Described below is a summary of experiments executed to determine the energetic stability and the chemical and radiation stability of SNL-A. These experiments were carried out to investigate the viability of SNL-A as a ceramic waste form phase, such as that which might be formed by thermal conversion of a Cs-exchanged silicotitanate ion exchanger.

Energetics of SNL-A. Using DFT total energy calculations, we optimized the positions of all the ionic coordinates and the shape of the unit cell as a function of volume in order to compare the energetics of the *Cc* and *C*2/*c* model solutions for SNL-A and that of the PNNL phase. At a given volume, the positions of the cations and the anions were determined by minimizing the Hellmann Feynman forces on the ions. The unit cell edges were determined by making adjustments, until the Pulay corrected stress tensor was zero. The structural parameters were considered to be fully relaxed when the forces on the ions were less that 0.005 eV/A and all stress tensor components were less than 0.001 eV/A^3. Calculations of this type were completed for a variety of volumes for each structure type. The resulting

(45) Malek, A.; Ozin, G. A.; Macdonald, P. M. *J. Phys. Chem.* **1996**, *100*, 16662.
(46) Ahn, M. K.; Iton, L. E. *J. Phys. Chem.* **1991**, *95*, 4496.
(47) Yagi, F.; Kanuka, N.; Tsuji, H.; Nakata, S.; Kita, H.; Hattori, H. *Microporous Mater.* **1997**, *9*, 229.

Table 6. Comparison of Rings of the SNL-A and PNNL Polymorphs of $Cs_2TiSi_6O_{15}$

phase [building blocks]	ring type	ring polyhedra[a]
SNL-A $Cs_2TiSi_6O_{15}$ (*Cc* polymorph)	3-ring	Si(2)−Si(4)−Ti Si(1)−Si(5)−Ti
[$Si(1)O_4$, $Si(2)O_4$, $Si(3)O_4$, $Si(4)O_4$,	5-ring	Si(2)−Si(1)−Si(5)−Si(4)−Si(6)
$Si(5)O_4$, $Si(6)O_4$, TiO_6]		Si(2)−Si(1)−Si(3)−Si(5)−Si(4)
	5-ring	Ti−Si(2)−Si(1)−Si(3)−Si(6)
		Ti−Si(1)−Si(2)−Si(6)−Si(3)
	6-ring	Ti−Si(1)−Si(3)−Ti−Si(6)−Si(2)
	7-ring	Ti−Si(3)−Si(5)−Ti−Si(2)−Si(6)−Si(4)
		Ti−Si(6)−Si(4)−Ti−Si(1)−Si(3)−Si(5)
	8-ring	Si(1)−Si(3)−Si(6)−Si(4)−Si(2)−
		Si(6)−Si(3)−Si(5)
PNNL $Cs_2TiSi_6O_{15}$[14] (*C*2/*c* polymorph)	3-ring	Si(2)−Si(3)−Ti
[$Si(1)_2O_7$, $Si(2)O_4$, $Si(3)O_4$, TiO_6]	5-ring	Si(2)−Si(3)−Si(1)−Si(2)−Si(3)
	5-ring	Ti−Si(2)−Si(3)−$Si(1)_2$
	6-ring	Ti−Si(1)−Si(3)−Ti−Si(1)−Si(3)
	8-ring	$Si(1)_2$−Si(2)−Si(3)−$Si(1)_2$−Si(3)−Si(2)
	8-ring	Ti−Si(2)−Si(1)−Si(3)−Ti−Si(2)−Si(1)−Si(3)

[a] Si(x) = Si(x)O_4; $Si(1)_2$ = $Si(1)_2O_7$; Ti = TiO_6.

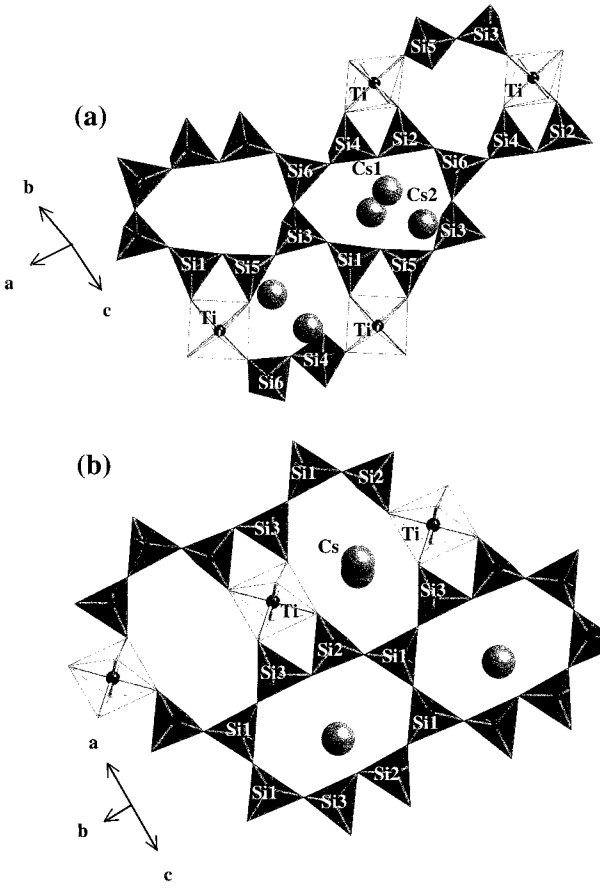

Figure 6. Views of (a) SNL-A on the (011) plane and (b) the PNNL phase on the (101) plane. These views reveal the major difference between the ring geometries of the two polymorphs: SNL-A has a seven-membered ring (2 Ti, 5 Si), whereas the PNNL phase has an eight-membered ring (2 Ti, 6 Si). Some of the Cs atoms are removed for ease of viewing.

energies were fit to a Birch[48] equation of state

$$E = a_0 + a_1V^{-2/3} + a_2V^{-4/3} + a_3V^{-6/3} \qquad (1)$$

which was used to determine the pressure, the bulk modulus (B_0), and the pressure derivative of the bulk modulus (B_0'). To estimate with some degree of confidence the small energy differences between these structures, a kinetic energy cutoff of 500 eV was used. The Brillouin zone integration was completed using a [222] Monkhorst−Pack type grid which reduced to 3 *k*-points in the irreducible Brillouin zone.[49−51] The results of these calculations are shown in the plot in Figure 9. These results show that the *Cc* solution is energetically favorable, as compared to the *C*2/*c* solution for SNL-A. In agreement with the NMR data and Rietveld refinement data, these calculations provided further evidence for the *Cc* model as the correct structure for SNL-A. Finally, the cohesive energy of SNL-A is found to be lower (higher stability) than the PNNL *C*2/*c* polymorph.

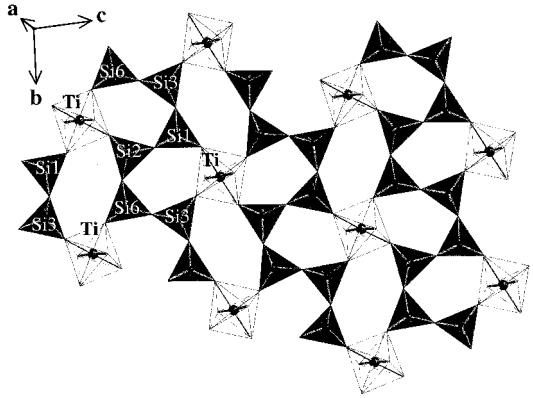

Figure 7. View of SNL-A, approximately down the *a*-axis, emphasizing the five-membered rings (1 TiO_6, 4 SiO_4) and six-membered rings (2 TiO_6, 4 SiO_4). (A similar view of the PNNL polymorph containing the same ring types is viewed down its *b*-axis.) The Cs atoms are removed for ease of viewing.

Chemical Durability of SNL-A. SNL-A shows extreme durability in aggressive chemical and radiation environments. The durability of SNL-A with respect to Cs leachability is shown in Figure 10, where leach rate is plotted as a function of leach time. Less than 0.2% Cs is lost from the original 37 wt % Cs composition, which translates as essentially no Cs lost due to leaching. Furthermore, SNL-A did not undergo any phase change as a result of the PCT leach tests, as determined by powder X-ray analysis of the leached samples. Addition-

(48) Birch, F. *J. Geophys. Res.* **1978**, *83*, 1257.

(49) Bouckaert, L. P.; Smoluchowski, R.; Wigner, E. *Phys. Rev.* **1936**, *50*, 58.

(50) Monkhorst, H. J.; Pack, J. D. *Phys. Rev. B.* **1976**, *13*, 5188.

(51) Evarestov, R. A.; Smirnov, V. P. *Phys. Status Solidi* **1983**, *119*, 9.

Table 7. Observed and Calculated ^{29}Si NMR Shifts and Related Structural Data for SNL-A

obsd ^{29}Si NMR peak shifts			^{29}Si NMR peak shifts calcd from DFT-optimized *Cc* model			^{29}Si NMR peak shifts calcd from SiO constrained *Cc* Rietveld model		
Si(x)	δ_{obs} (ppm)	peak integratn (% of tot.)	δ_{calc} (ppm)	av S i(x)−O− Si(y) angle (deg)	Si(x)− O−Ti angle (deg)	δ_{calc} (ppm)	av S i(x)−O−Si(y) angle (deg)	Si(x)− O−Ti angle (deg)
Si(1)	−96.8	16.3	−95.1	140	135	−94.9	145	133
Si(4)	−97.8	19.6	−96.0	141	134	−96.2	145	132
Si(2)	−100.2	17.9	−97.7	142	134	−97.5	144	134
Si(5)	−102.4	15.5	−101.6	147	139	−106.9	154	154
Si(6)	−107.3	15.5	−106.5	150	146	−107.1	154	143
Si(3)	−110.0	15.2	−109.6	154	156	−107.8	150	149

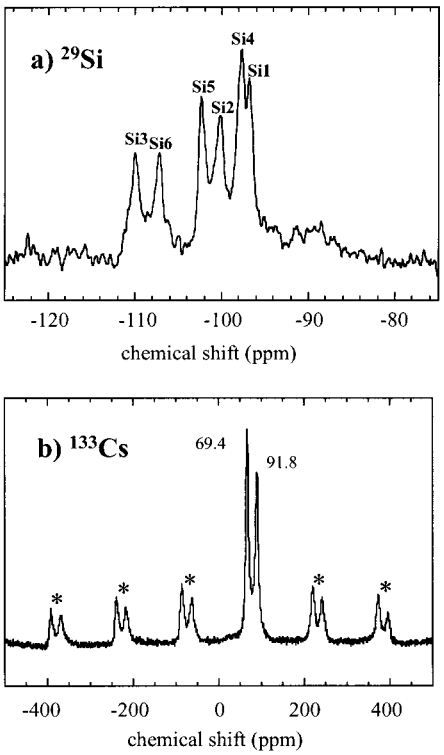

Figure 8. (a) ^{29}Si MAS NMR of SNL-A showing 6 unique Si Q^3 (3 Si, 1 Ti) sites, all of equal integrated area. (b) ^{133}Cs MAS NMR of SNL-A showing two unique Cs sites in a 1:1 ratio. Asterisks indicates spinning sidebands.

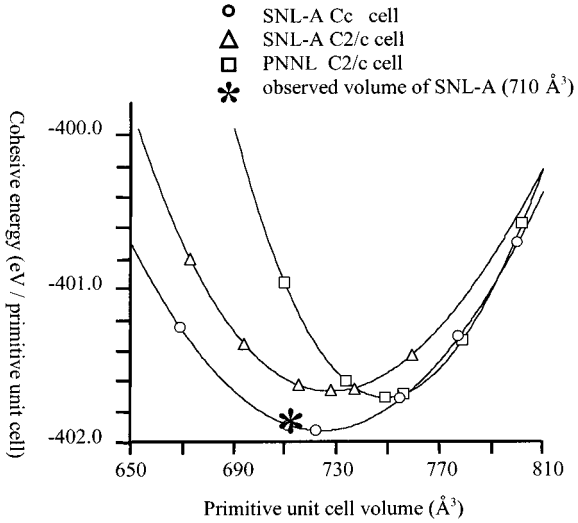

Figure 9. Cohesive energy (eV/primitive cell) as a function of primitive unit cell volume, calculated for the SNL-A *Cc* solution, the SNL-A *C*2/*c* solution, and the *C*2/*c* PNNL $Cs_2TiSi_6O_{15}$.

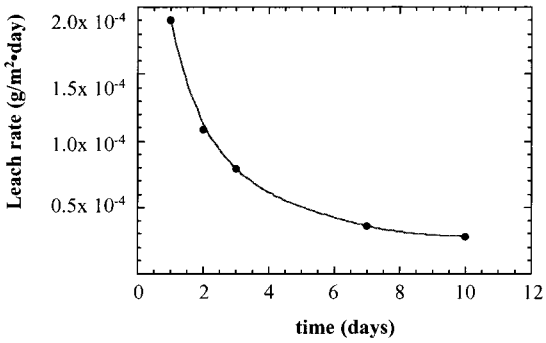

Figure 10. Product consistency test (PCT) leach test for SNL-A showing Cs leach rate as a function of time.

ally, attempted ion exchange experiments (3 days at 90 °C) in (1) 1 M aqueous sodium chloride solution and (2) 1 M aqueous sodium hydroxide solution resulted in no ion exchange and no structural change.

Radiation Durability of SNL-A. Radiation stability determination of all Cs silicotitanate phases synthesized in the collective (SNL/PNNL/UC Davis) study is important in order to assess the durability of the phases for ion exchange with radionuclides or waste form applications. Electron irradiation with in situ TEM studies have proven to be useful in simulating the effects of radiation damage caused by fission products.[16,52,53] SNL-A is extremely radiation resistant. This technique reveals the extent and mechanism of radiation damage on an atomic level, which can be extrapolated to a pure bulk material such as SNL-A. Figure 11 shows the electron diffraction pattern of SNL-A, before and after cumulative radiation dose of 5×10^{23} electrons/cm^2. No changes in the diffraction pattern resulting from irradiation induced amorphization are observed.

Summary and Conclusions

Phase searches by hydrothermal treatment (120−200 °C) of $Cs_2O-SiO_2-TiO_2-H_2O$ precursor mixtures have produced a new *Cc* polymorph of $Cs_2TiSi_6O_{15}$ (SNL-A). SNL-A is stable up to its melting temperature at 1150 °C; upon cooling, a glass is formed. No interconversions between the *Cc* SNL-A and *C*2/*c* PNNL polymorphs are observed. The two polymorphs are similar in their unit cell dimensions and identical in melting temperature. However, distinctions are seen in the $Si_2O_5^{2-}$ layers and polyhedral ring structures. SNL-A possesses a seven-membered ring which is not observed in the *C*2/*c* PNNL

(52) Wang, L. M.; Wang, S. X.; Ewing, R. C. *Radiation Effects in Zeolite: Relevance to near-field contamination*; Las Vegas, NV, 1997; p 772.

(53) Wang, L. M.; Wang, S. X.; Gong, W. L.; Ewing, R. C.; Weber, W. J. *Mater. Sci. Eng.* **1998**, *A253*, 106.

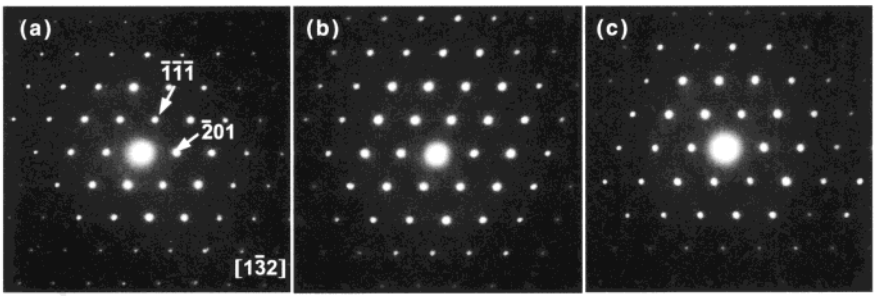

Figure 11. Electron irradiation of SNL-A showing its extreme radiation durability: (a) before irradiation; (b) 5.8×10^{21} electron/cm^2; (c) 7.9×10^{21} electrons/cm^2. The dose in (c) is equivalent to an energy deposition of 2.1×10^{12} Gy and a displacement damage of ~0.1 dpa (displacements/atom). The sample was irradiated at a dose rate of 1.8×10^{12} electrons /(s·cm^2).

polymorph, and the *C*2/*c* PNNL polymorph has an eight-membered ring which is not found in SNL-A.

The structure of SNL-A is close to centrosymmetric; the Rietveld refinement of SNL-A powder X-ray diffraction data provided a relatively satisfactory model in the space group *C*2/*c*. However, both ^{133}Cs and ^{29}Si MAS NMR spectroscopy suggested twice as many unique crystallographic sites for Cs and Si than this solution predicted. DFT total energy calculations were applied to optimize both the *Cc* and *C*2/*c* model structures. The DFT total energy calculations showed the cohesive energy for the *Cc* solution for SNL-A to be lower than that of the *C*2/*c* solution, which again suggests the *Cc* solution is correct. This approach gave a solution with better agreement indices and which agreed with the NMR data. Calculations of theoretical ^{29}Si NMR chemical shifts for SNL-A using both the DFT and Rietveld refinement results showed that the downfield chemical shift increases with increasing Si−O−X angle, where X is the neighboring Si or Ti. The chemical shifts calculated from the DFT data agree better with the observed shifts than those calculated from the Rietveld model.

These collective results have shown that use of integrated theory and experiment has allowed us to arrive at an excellent structural solution for SNL-A. Specifically, Rietveld structure refinement, density functional theory optimization, and solid-state ^{133}Cs and ^{29}Si NMR were all necessary to obtain the most accurate description of a complex phase (of which single crystals of suitable size are not presently obtainable), which has a unit cell containing 24 crystallographically unique atoms.

Finally, leach tests and irradiation experiments showed SNL-A to be extremely resistant to both structural damage and Cs loss by either method. These results suggest that SNL-A is a viable silicotitanate phase for ceramic waste forms, such as for immobilization of radioactive ^{137}Cs. Furthermore, DFT total energy calculations showed the cohesive energy for *Cc* SNL-A to be lower and, thus, energetically favorable within the constraints of the model, relative to the high temperature *C*2/*c* PNNL polymorph. Since the SNL-A polymorph of $Cs_2TiSi_6O_{15}$ is favored under hydrothermal synthesis conditions (≤200 °C) and the PNNL polymorph is favored by high-temperature routes, it is expected that kinetics rather than thermodynamics dictate the formation of these two phases. In ongoing work, we are investigating the relative stability of the two $Cs_2TiSi_6O_{15}$ polymorphs using high-temperature oxide melt calorimetry,[54] where the enthalpies of formation from oxides for these phases will be determined.

Acknowledgment. This work was supported by the U.S. DOE under Contracts DE-AC04-94AL85000 (Sandia National Laboratories) and W-7405-Eng-48 (University of California Lawrence Livermore National Laboratory). SNL and University of Michigan authors thank the DOE Environmental Management Science Program (EMSP) for funding for this work under separate grants for the University of Michigan and SNL (EMSP Grant DE-FG07-97ER45652 at the University of Michigan; Project No. 27601 at SNL). We thank Dr. Todd Alam at Sandia National Laboratories for the preliminary NMR spectroscopy experiments and M. Lou Balmer (PNNL), Yali Su (PNNL), Alex Navrotsky (UC Davis), and Hongwu Xu (UC Davis) for helpful discussions.

CM000259G

(54) Navrotsky, A. *Phys. Chem. Miner.* **1997**, *24*, 222.